15 June 1998

Optics Communications

Optics Communications 152 (1998) 198–206

Full length article

Dynamics of optical vortex solitons

Yuri S. Kivshar [a], Jason Christou [b], Vladimir Tikhonenko [b], Barry Luther-Davies [b], Len M. Pismen [c]

[a] *Optical Sciences Centre, Australian Photonics Cooperative Research Centre, Research School of Physical Sciences and Engineering, Australian National University, ACT 0200 Canberra, Australia*

[b] *Laser Physics Centre, Australian Photonics Cooperative Research Centre, Research School of Physical Sciences and Engineering, Australian National University, ACT 0200 Canberra, Australia*

[c] *Department of Chemical Engineering, Technion-Israel Institute of Technology, 32000 Haifa, Israel*

Received 16 October 1997; revised 9 March 1998; accepted 10 March 1998

Abstract

We analyse the drift of an optical vortex soliton created on a slowly diffracting, finite-extend background field. In the framework of the generalized nonlinear Schrödinger equation we derive the motion equation describing the change of the vortex velocity induced by local gradients of the phase and intensity of the background field. We present experimental measurements of the motion of a vortex soliton, created by a phase mask in a diffracting Gaussian laser beam passed through a nonlinear saturable medium. The experimental results are shown to be in good agreement with our theoretical model and corresponding numerical simulations carried out for both Kerr and saturable media with experimentally determined initial conditions. © 1998 Elsevier Science B.V. All rights reserved.

PACS: 42.65.Jx; 42.50.Rh; 42.65.Hw

1. Introduction

Spatio-temporal evolution of light in nonlinear media and stable propagation of temporal and spatial optical solitons have been subjects of considerable theoretical and experimental research in nonlinear optics during recent years. Localized solutions of the nonlinear propagation equations when a background wave is modulationally stable are *dark solitons*, observable as intensity dips within a uniform background. Temporal dark solitons described by the $(1+1)$-dimensional (one temporal and one spatial) nonlinear Schrödinger equation (NLS) have been predicted theoretically [1] and subsequently observed in optical fibres [2]. The spatial analogues of these dark solitons were also observed experimentally as spatial dark stripe solitary waves in a bulk nonlinear medium [3]. Despite strong similarities between dark stripes and their temporal relatives, the stripe differs from the temporal soliton in that it is unconstrained along the extra transverse spatial dimension, whereas the temporal soliton is confined by the fibre in higher transverse dimensions. Linear stability analysis developed for a defocusing Kerr medium [4] shows that a spatial dark soliton stripe is *unstable* to transverse (long-wavelength) modulations. This transverse modulational instability has been already observed experimentally for saturable [5] and photorefractive [6] media [1]. In the strongly nonlinear regime, the instability leads to the gen-

[1] The authors of Ref. [6] claim that the transverse (or 'snake-type') instability should always exist for photorefractive solitons. However, the recent theoretical results (see Ref. [19]) suggest that the transverse instability of a soliton stripe is suppressed in a saturable medium, as it should be for the case of photorefractive solitons. Therefore, the instability reported by Mamaev et al. may be also associated with the increase of nonlinearity beyond the threshold of soliton formation. It should be also noticed that the existence of stable and robust $(1+1)$-dimensional soliton stripes in a photorefractive medium has been demonstrated independently by Z. Chen et al. [7].

PII S0030-4018(98)00149-7

eration of pairs of optical vortex solitons with alternating polarities. The instability induced evolution of $(1+1)$-dimensional stripe beams and generation of vortices have been investigated both numerically [8,9] and using asymptotic analytical theory [10].

Optical vortex solitons are stable stationary structures which exist in a defocusing bulk nonlinear optical medium on a uniform background. Vortex soliton solutions of the $(2+1)$-dimensional cubic nonlinear Schrödinger equation were introduced and analysed in the pioneering paper by Pitaevskii [11] as topological excitations within superfluids. In the context of nonlinear optics, they were theoretically suggested by Snyder et al. [12] and experimental observations of optical vortex solitons have been reported by several groups [13–21] for different optical materials. In experiments, however, vortex solitons are observed for different types of initial conditions. So far, the vortex solitons that reside on 'infinite' background beams have been only generated by Z. Chen et al. [17,18]. In most of the other cases, the vortex solitons have been created by finite total energy and reside within the nonuniform background. As a result, vortex motion is observed to be strongly dependent on the inhomogeneities in the background field, diffracting even stronger in the presence of a defocusing nonlinearity. This is quite different from what we can learn from the theory of vortex solitons. Indeed, the theory of optical vortex solitons developed to date assumes a background of constant amplitude (analogous to fluid incompressibility), and is unable to capture a number of interesting features of vortex dynamics, e.g. the drift and rotation of a vortex around the beam center – effects which also exist for linear propagation but become dependent on light intensity in the nonlinear regime. Understanding this dynamics is important for future application of vortex solitons in steerable all-optical switching devices based on the concept of light-guiding-light.

In this paper we develop, for the first time to our knowledge, a theory of optical vortex motion on an inhomogeneous background field and compare our analytical and numerical results with those obtained experimentally. The theory we suggest here is rather general, and it can be applied to different physical situations when the background field evolves slowly in comparison with the vortex parameters. However, in the present paper we concentrate on the case of a diffracting background beam which can be easily verified experimentally and numerically.

The paper is organised as follows. In Section 2 we begin with the generalised NLS equation which is the model characterising our physical system. Looking for localised vortex solutions within a slowly varying field, we derive a nonlinear equation that allows the effects of background non-uniformity to be incorporated into a problem of the vortex motion, induced by gradients of the background field. The resulting equation is similar to a previous analysis carried out in the context of a superfluid model [22]. In Section 3 we apply the method of matched asymptotic expansion to derive an equation of motion for the vortex core. The equation of motion is readily interpreted and is shown to describe the behaviour seen in experiments and simulations. In particular, it predicts the source of vortex radial drift and rotation in a beam to be due to background gradients of phase and intensity respectively. In Section 4 we discuss experimental results and compare them with theory and numerical simulations, demonstrating a reasonably good agreement. Finally, a discussion in Section 5 summarises and concludes the paper.

2. Model

We consider the propagation of a monochromatic scalar electric field $\mathscr{E}$ in a bulk optical medium with an intensity-dependent refractive index, $n = n_0 + n_{\rm nl}(I)$, where n_0 is the uniform refractive index of the unperturbed medium, and $n_{\rm nl}(I)$ describes the change in the index due to the field intensity $I = |\mathscr{E}|^2$. In the so-called paraxial approximation, Maxwell's equations can be reduced to the generalised NLS equation for the slowly varying envelope $E(z,\boldsymbol{r}) = \mathscr{E}(z,\boldsymbol{r})\exp(ik_0 n_0 z)$ of the electric field,

$$-2ik_0 n_0 \frac{\partial E}{\partial z} + \nabla^2 E + g(I)E = 0, \tag{1}$$

where k_0 is the free-space wave number, n_0 is the linear refractive index, $I = |E|^2$ is the beam intensity, and ∇ is a gradient operator defined with respect to the transverse coordinates $\boldsymbol{r} = (x,y)$. The function $g(I) = 2k_0^2 n_0 n_{\rm nl}(I)$ describes the nature of the nonlinearity, and is determined by the intensity-dependent correction $n_{\rm nl}(I)$ to the refractive index. Analysing the modification of a vortex soliton by a variation of the *background field*, we look for solutions of Eq. (1) in the form (see Ref. [23] where a similar approach was used for a dark soliton)

$$E(z,\boldsymbol{r}) = \sqrt{I_b}\, e^{i\theta_b} \upsilon(z,\boldsymbol{r})$$

and assume that the background field with the intensity $I_b(z,\boldsymbol{r})$ and phase $\theta_b(z,\boldsymbol{r})$ satisfies Eq. (1). This yields the equation for the auxiliary field $\upsilon(z,\boldsymbol{r})$,

$$-2ik_0 n_0 \frac{\partial \upsilon}{\partial z} + \nabla^2 \upsilon + \left[g\left(I_b|\upsilon|^2 \right) - g(I_b) \right] \upsilon = -\nabla \upsilon \cdot \boldsymbol{f}, \tag{2}$$

where the complex vector $\boldsymbol{f}$ is defined by the evolution of the background field,

$$\boldsymbol{f} = \boldsymbol{f}^r + i\boldsymbol{f}^i \equiv \nabla \ln I_b + 2i\nabla\theta_b, \tag{3}$$

and the boundary condition $|\upsilon| \to 1$ applies for large $|\boldsymbol{r} - \boldsymbol{r}_0|$, where the position of the vortex core $\boldsymbol{r}_0$ is defined as $\upsilon(\boldsymbol{r}_0) = 0$.

In the particular case of a defocusing Kerr medium, i.e. when $n_{nl}(I) = -n_2 I$, Eq. (2) takes the form of a perturbed NLS equation

$$-2ik_0 n_0 \frac{\partial v}{\partial z} + \nabla^2 v + 2k_0^2 n_0 n_2 I_b \left(1 - |v|^2\right) v = -\nabla v \cdot \boldsymbol{f}. \tag{4}$$

In the derivation that follows, we use this perturbed form of the NLS equation to describe the evolution of the auxiliary field, and thereby obtain an equation of motion for the vortex core.

3. Vortex equation of motion

In this section, we apply the method of matched asymptotic expansions to the analysis of a slow vortex motion in a shallow gradient of the background field. The expansion near and far from the vortex core will be followed by asymptotic matching at an intermediate distance. We mostly follow a similar analysis in Ref. [22] that, in its turn, draws on the application of the same technique in other settings [24–26].

3.1. Asymptotic expansion near the vortex core

We assume that the function v describes a vortex with the centre coordinate $\boldsymbol{r}_0(z)$, and the fields I_b and θ_b vary slowly in comparison with the vortex scales. This means that gradients of these fields produce a small parameter ϵ. It is expected that the shift of the vortex will be of the same order of magnitude. Then, the problem is to describe a change of the position of the vortex (i.e., the so-called *vortex drift*) for the field v under the action of these slowly varying background fields. To clarify the idea of a 'background field', one may picture it as the field which would exist if the vortices were somehow removed. We rescale to dimensionless coordinates by using the value of the *slowly varying* background field at the vortex centre, $I_0 = I_b(\boldsymbol{r}_0)$, so that $z \to -z/(k_0 n_0 n_2 I_0)$ and $\boldsymbol{r} \to \boldsymbol{r}/(k_0 n_0 \sqrt{2n_2 I_0/n_0})$, then set $\boldsymbol{f} = \epsilon \boldsymbol{F}$ where $|\boldsymbol{F}| = \mathrm{O}(1)$. In this case Eq. (4) becomes

$$i\frac{\partial v}{\partial z} + \nabla^2 v + \frac{I_b}{I_0}\left(1 - |v|^2\right) v = -\epsilon \nabla v \cdot \boldsymbol{F}, \tag{5}$$

where $\boldsymbol{F}$ has also been rescaled. The vortex velocity, in this new coordinate scale, is assumed to be small, producing the same small parameter ϵ as the background gradients, so that

$$\frac{\mathrm{d}\boldsymbol{r}_0}{\mathrm{d}z} = \boldsymbol{w} = \epsilon \boldsymbol{V}, \tag{6}$$

where $|\boldsymbol{V}| = \mathrm{O}(1)$.

Next, we solve Eq. (5) in the vicinity of the vortex core in the reference frame moving with the vortex drift velocity $\boldsymbol{w}$. Since the background field does not change significantly on the scale of the core, the term I_b/I_0 should be expanded as

$$I_b/I_0 \approx 1 + \boldsymbol{r}\cdot\nabla \ln I_b|_{\boldsymbol{r}=r_0} \equiv 1 + \epsilon \boldsymbol{r}\cdot \boldsymbol{F}_0^r, \tag{7}$$

where the rescaled complex vector $\boldsymbol{F}_0$ is calculated at the position of the vortex, $\boldsymbol{F}_0 \equiv \boldsymbol{F}|_{\boldsymbol{r}=r_0}$. Thus, Eq. (5) becomes

$$\nabla^2 v + \left(1 - |v|^2\right) v = \epsilon\Big[\left(i\boldsymbol{V} - \boldsymbol{F}\right)\cdot\nabla v - \boldsymbol{r}\cdot\boldsymbol{F}_0^r\left(1 - |v|^2\right) v\Big]. \tag{8}$$

We expand also the field v as $v = v_0 + \epsilon v_1 + \dots$ and substitute the asymptotic series into Eq. (8). In the zero-order approximation in ϵ we find the standard nonlinear (stationary cubic NLS) equation which defines the vortex profile

$$\nabla^2 v_0 + \left(1 - |v_0|^2\right) v_0 = 0, \tag{9}$$

so that, in the polar coordinates of the moving frame, its solution is given by the expression

$$v_0 = \rho(r)\,\mathrm{e}^{im\phi} \tag{10}$$

where $m = \pm 1$ is the vortex charge (polarity), and the function $\rho(r)$ that verifies

$$\frac{\mathrm{d}^2\rho}{\mathrm{d}r^2} + \frac{1}{r}\frac{\mathrm{d}\rho}{\mathrm{d}r} + \left(1 - \frac{1}{r^2} - \rho^2\right)\rho = 0 \tag{11}$$

is the well known vortex amplitude profile, first studied in the superfluid context, and known numerically [11] (see also Ref. [27] and references therein).

The first-order approximation yields the inhomogeneous equation,

$$\mathscr{L}(v_1, v_1^*) = \Psi(\boldsymbol{r}) \tag{12}$$

with the homogeneous part

$$\mathscr{L}(v_1, v_1^*) = \nabla^2 v_1 + v_1 - 2|v_0|^2 v_1 - v_0^2 v_1^*, \tag{13}$$

and the right-hand-side part

$$\Psi(\boldsymbol{r}) = (i\boldsymbol{V} - \boldsymbol{F}_0)\cdot\nabla v_0 - \boldsymbol{r}\cdot\boldsymbol{F}_0^r\left(1 - |v_0|^2\right) v_0. \tag{14}$$

Using Eq. (10) brings Eq. (14) to the form

$$\Psi(\boldsymbol{r}) = \left\{\frac{m}{r^2}\rho(r)(\boldsymbol{V} + i\boldsymbol{F})\times\boldsymbol{r} + \frac{1}{r}\frac{\mathrm{d}\rho(r)}{\mathrm{d}r}(i\boldsymbol{V} - \boldsymbol{F})\cdot\boldsymbol{r} - \left[1 - \rho(r)^2\right]\rho(r)\boldsymbol{F}^r\cdot\boldsymbol{r}\right\}\mathrm{e}^{im\phi}. \tag{15}$$

We omit here the index '0', presuming that the value of the effective 'force' $\boldsymbol{F}$ is taken at the vortex core, $\boldsymbol{r} = r_0$.

The solvability condition of the first-order equation (12), (15) means the orthogonality of the inhomogeneous part, $\Psi(\boldsymbol{r})$, to the two components of the translational eigenfunction, ∇v_0^*, of the adjoint homogeneous equation. We proceed in the usual way [22], taking the product with the eigenfunction and integrating by parts. In order to avoid divergences in the far field, the integration is over a circle with a *finite* large radius $L = O(\epsilon^{-1/2}) \gg 1$, and the contour integrals *do not vanish*:

$$\mathrm{Re}\left\{ \int_0^L r\,\mathrm{d}r \int_0^{2\pi} \mathrm{d}\phi\, \nabla v_0^* \Psi(\boldsymbol{r}) - L \int_0^{2\pi} \mathrm{d}\phi \left(\nabla v_0^* \cdot \partial_r v_1 - v_1 \cdot \partial_r \nabla v_0^* \right)_{r=L} \right\} = 0. \quad (16)$$

We take the direction of $\boldsymbol{F}^r$ as the y axis; then the normal direction is the x axis. The projection on the x and y components of the translational eigenfunction yields the following expressions for the area integrals:

$$I_x = -m\pi\left(V_y - F_y^i\right),$$
$$I_y = m\pi\left[\left(V_x - F_x^i\right) - mF^r(I_1 + I_2)\right], \quad (17)$$

where

$$I_1 = \int_0^L r^2\left[1 - \rho^2(r)\right]\, \rho(r)\, \frac{\mathrm{d}\rho}{\mathrm{d}r}\,\mathrm{d}r = \int_0^L \left\{ \rho(r)\, \frac{\mathrm{d}\rho}{\mathrm{d}r} - r\frac{\mathrm{d}\rho}{\mathrm{d}r}\frac{\mathrm{d}}{\mathrm{d}r}\left(r\frac{\mathrm{d}\rho}{\mathrm{d}r}\right)\right\}\mathrm{d}r = \tfrac{1}{2} \quad (18)$$

has been computed using Eq. (11) then integrating by parts, and

$$I_2 = \int_0^L \left\{ \tfrac{1}{2}\rho^2(r) + r\left(\frac{\mathrm{d}\rho}{\mathrm{d}r}\right)^2 \right\} = \ln(L/c), \quad (19)$$

with $c \approx 1.126$, has been found numerically. The x-component is non-divergent, and can be cancelled exactly by setting $V_y = F_y^i$.

The contour integral in Eq. (16) depends on the asymptotics of the first-order field v_1. Since $\rho_0(L) \propto [1 - O(\epsilon)]$, the contour integral can be expressed, to the leading order, through the phase field only. This can be done in two ways: first, as the outer asymptotics of the inner solution for the first-order correction v_1, and second, as the inner asymptotics of the far field solution. It can be shown that the leading term in the asymptotics of the phase correction, obtained by solving Eq. (12), is $\theta_1(r) \propto r \ln(\alpha r)\cos\phi$, where the parameter α should be found by matching with the outer solution. The use of the solvability condition shortcuts actually solving the first-order equation (12).

3.2. Far-field expansion and matching

According to the method of matched asymptotics, now we should match the expansion near the vortex core with the outer expansion for large r. This means that we should compute the far-field correction to the background field, and take its inner limit, that *must* give a value of the contour integral $\propto F^r \ln L$ to match the inner solution and cancel the divergence of I_2. Eq. (5) has to be rewritten in the coordinate frame $\boldsymbol{X} = \epsilon \boldsymbol{x}$ extended by the factor ϵ. After setting $v = \rho\, \mathrm{e}^{i\theta}$, the real and imaginary parts are separated as usual giving, respectively, the Bernoulli and the continuity equation. The former gives in the leading order just $\rho = 1$, and the latter gives the phase equation

$$\hat{\nabla}^2\theta + \boldsymbol{F}\cdot\hat{\nabla}\theta = 0, \quad (20)$$

where $\hat{\nabla}$ is the gradient with respect to the extended variable. This should be, strictly speaking, solved with a *position-dependent* $\boldsymbol{F}^r = \hat{\nabla} \ln I_b$, subject to the circulation condition relative to the instantaneous vortex position.

The solution with constant $\boldsymbol{F}^r$, which we assume to be directed along the Y axis, is expressed [22] as

$$\theta_X = -m\left(\Phi_Y + \Phi F^r\right), \quad \theta_Y = m\Phi_X, \quad (21)$$

where Φ satisfies the equation

$$\hat{\nabla}^2\Phi + \Phi_Y F^r = 2\pi\delta(\boldsymbol{r} - r_0), \quad (22)$$

and it can be therefore found in the form

$$\Phi = -\exp\left(-\frac{F^r R}{2}\sin\phi\right) K_0\left(\frac{RF^r}{2}\right), \quad (23)$$

where $R = \epsilon r$ is the extended radial coordinate and $K_0(x)$ is a modified Bessel function. The inner asymptotics of θ following from this solution is

$$\theta = m\phi - \frac{m}{2}RF^r\cos\phi \ln\left|\frac{RF^r\,\mathrm{e}^{\gamma}}{4}\right|, \quad (24)$$

where γ is the Euler constant ($\gamma \approx 0.577$). For matching, it has to be rewritten using the *inner* scaling; then R is replaced on the matching contour by ϵL.

Returning to the contour integral in Eq. (16), we take note that terms decaying faster than $1/r$ vanish in the limit $L \to \infty$ and can be neglected. Terms surviving the integration over the circle appear only in the y component of the solvability condition. Using Eqs. (24), (17) and (19), the y component of the solvability condition (16) now becomes

$$m\pi\left\{ V_x - F_x^i - mF^r\left[\tfrac{1}{2} + \ln(L/c) - \ln\left|\frac{L\,\mathrm{e}^{\gamma+1/2}}{4}\epsilon F^r\right|\right]\right\} = 0. \quad (25)$$

Collecting all the results and removing the book-keeping parameter ϵ, we can present the solvability conditions for the two components in a vector form

$$\boldsymbol{w} = \boldsymbol{f}_0^i + m\boldsymbol{J}f_0^r \ln\left(\frac{c|\boldsymbol{f}_0^r|\,\mathrm{e}^{\gamma}}{4}\right), \quad (26)$$

where, for simplicity, we introduce the operator of rotation by $\pi/2$, $\boldsymbol{J}$, which is defined by the matrix

$$\boldsymbol{J} = \begin{pmatrix} 0 & -1 \\ 1 & 0 \end{pmatrix},$$

and the force components, $\boldsymbol{f}$, are defined by Eq. (3), but evaluated at the vortex core.

In the dimensional units which we use below to compare with the experimental results, the motion equation for the vortex core can be presented, by recovering the physical scaling in Eq. (26), as the following,

$$k_0 n_0 \frac{\mathrm{d}\boldsymbol{r}_0}{\mathrm{d}z} = \left(-\nabla\theta_b + \frac{m}{2} C\boldsymbol{J}\nabla\ln I_b \right)\bigg|_{\boldsymbol{r}=r_0}, \tag{27}$$

where $\boldsymbol{J}$ is the operator introduced above, and C is a slowly varying function of I_b. In the particular case of the Kerr medium, the coefficient C has been derived above:

$$C = -\ln\left(\frac{ce^{\gamma}|\nabla\ln I_b|}{4k_0 n_0\sqrt{2n_2 I_0/n_0}} \right)$$

but in the general case of non-Kerr medium we can expect a similar form of the motion equation, as described below.

It is important to mention that the derivation of the analytical model presented above, even being asymptotically rigorous, is applicable only for weak inhomogeneities of the background field. As a result, the parameters formally corresponding to negative values of the coefficient C, including the limit $C \to 1$, are beyond the applicability limits of the asymptotic methods (i.e. the logarithm of a large quantity does not change sign within the approximation adopted).

3.3. Extension to a general case of non-Kerr medium

For a general function $g(I)$ in Eq. (2), the coordinates are rescaled by $g(I_0)$ rather than I_0 as before, and Eq. (5) becomes

$$i\frac{\partial v}{\partial z} + \nabla^2 v + \frac{g(I_b)}{g(I_0)}\left[1 - \frac{g\left(|v|^2 I_b\right)}{g(I_b)}\right] v = -\epsilon\nabla v \cdot \boldsymbol{F}. \tag{28}$$

Expanding as in Eq. (7) and proceeding exactly as in the Kerr case gives in the zero-order a modified equation for the stationary vortex profile

$$\nabla^2 v_0 + \left(1 - G\left(|v_0|\right)^2\right) v_0 = 0, \tag{29}$$

where $G(x) = g(I_0 x)/g(I_0)$. In the first-order approximation Eq. (12) is again obtained, but with a modified coefficient on the $\boldsymbol{r}\cdot F_0^r$ term. Thus, all results are obtained as before with a modified numerical coefficient c in Eq. (19) and with a rescaled coefficient

$$C = -\ln\left(\frac{ce^{\gamma}|\nabla\ln I_b|}{4k_0 n_0\sqrt{2n_{nl}(I_0)/n_0}} \right)$$

In particular, for the important case of a saturable nonlinearity we take

$$g(I) = \frac{I}{1+sI},$$

where the dimensionless parameter s characterises the inverse saturation intensity relative to the background intensity; larger values of s correspond to a stronger saturation of the nonlinearity. Calculation of the coefficient c for this model yield $c = 1.126$ at $s = 0$ (non-saturable case), $c = 1.412$ at $s = 1$, and $c = 1.639$ at $s = 2$.

3.4. Prediction of vortex motion

As follows from the analysis presented above, to describe the vortex drift induced by the diffracting background field, one should know the evolution of this field a priori, so that the radial and angular velocity components for the vortex motion can be calculated according to Eq. (27). It is implicit in the chosen assumptions of scale that the background field in the absence of the vortex evolves in approximately the same manner as it would when hosting a vortex. Thus, even qualitative knowledge of the propagation behaviour of a field may be used, along with the vortex equation of motion, to predict the action upon a vortex subsequently nested in that field. The following example of a vortex nested in a Gaussian beam serves to illustrate how vortex motion may be simply predicted.

The transverse ‘velocity’ of a vortex, according the model (27), has two components arising separately from the transverse phase and intensity gradients of its background field, evaluated at the position of the vortex. The first component, $-\nabla\theta_b$, is directed normal to the wavefront of the background, that is in the direction of transverse energy flow in the background field, giving rise to *radial motion* of a vortex in a Gaussian beam. The second component, $\frac{1}{2}mC\boldsymbol{J}\nabla\ln I_b$, is directed along the intensity contour (isophote) of the background upon which the vortex is positioned, with the sense of direction given by the vortex charge, m. For a Gaussian background, the isophote in any transverse plane is a circle, and so the second component of velocity describes the *angular motion* of the vortex. The flattening of the intensity profile under nonlinear action reduces the intensity gradient and thus subtracts from the rotation experienced by a vortex in linear propagation. For flatter intensity profiles (plane waves), the motion of the vortex becomes more dependent on the background wavefront solely, and results of previous work which have examined this behaviour [28,29] may be recovered.

Qualitatively similar types of vortex behaviour, namely the vortex drifts induced by background field gradients, have been also observed in numerical simulations of spiral waves [31] within a system governed by the complex Ginzburg-Landau equation. However, no asymptotic theory has been developed in Ref. [31] in order to describe this behaviour analytically.

A simple analysis can be made for ‘beam-like’ fields employing a Gaussian ansatz to approximate the evolution of the background field in a self-defocusing medium.

Using the Gaussian ansatz, we can make explicit calculations in Eq. (27), and the resulting equations for the vortex core can be integrated to yield

$$r_0(z) = \frac{w(z)}{w(0)} r_0(0), \tag{30}$$

$$\phi(z) = \phi(0) + \frac{mC}{k_0 n_0} \int_0^z \frac{\mathrm{d}\zeta}{w^2(\zeta)}, \tag{31}$$

where the polar coordinates r_0 and ϕ characterise the vortex position at a propagation distance z. Here $w(z)$ is the beam radius which can be calculated by various methods [32]. These equations have been found to effectively characterise aspects of vortex behaviour important to the problem of vortex steering [33]. Although linear propagation is outside the parameters set in the derivation of the equation of motion, exact agreement is obtained, in this case, with vortex dynamics calculated by other methods [34], provided that $C \to 1$. Indeed, even self-focusing behaviour is qualitatively described for situations in which the background remains ‘beam-like’, that is, prior to the onset of beam collapse, though the form for C is not determined.

Experimental and numerical results also confirm that accurate qualitative predictions may be made using the model (27), even where the background deviates from the familiar plane wave or Gaussian form. For example, a black soliton stripe has isophotes which run parallel to the stripe and no transverse energy flow, suggesting that a vortex will travel parallel to the stripe with propagation. Of course, the soliton stripe is transversely unstable and its evolution is quite significantly altered by the presence of a vortex, thus taking this situation outside the descriptive limits of this model for vortex motion. However, with a vortex far enough away from the stripe, the onset of stripe instability may be delayed and the predicted parallel motion may be observed.

Vortex *interaction* is also adequately accounted for by considering the host beam for one vortex as being comprised of the underlying background field along with the remaining vortices. A single vortex has circular isophotes centred on the vortex core and also circular energy flow. Thus one vortex interacting with the background field generated by another will move in the direction normal to the line connecting its core with the background vortex. The situation is exactly the same reversing the roles of the vortices in the pair. The resultant motion of the vortex pair can therefore be only circular or parallel, depending on the vortex chirality. It is also possible to include the effect of a non-planar background in this picture, in order to estimate any influence on the observed interactions between vortices.

A simple physical argument underlies this form for the vortex equation of motion used in the above examples, which may clarify the mechanisms underlying vortex behaviour. Consider the ‘momentum’, $\int I \nabla\theta$, of a small element of the transverse field surrounding the vortex core. In the first case, assume that the intensity is uniform, then the momentum of the element is proportional to the sum of the vortex phase gradient around the core, which is zero, and the sum of the background phase gradient around the core. Thus the element around the core has a momentum approximately proportional to the background phase gradient at the vortex position, giving rise to the first velocity component in the equation of motion. In the second case, assume that the background phase is uniform, then the background phase gradient around the core is zero. The momentum of the element is thus proportional to the sum of the vortex phase gradient weighted by the background intensity, around the core. Using the ideas of vector summation, it is apparent that an imbalance in background intensity, over the small region around the vortex core, gives rises to a net momentum component in the direction normal to the intensity gradient, i.e. along the isophote, sourcing the second velocity component in the equation of motion.

We can also draw the reader’s attention to several analogies with the problem of the fluid vortex motion. Indeed, employing the language of the fluid mechanics and using the analogy between the superfluid (i.e. described by the NLS equation) and classical vortices (see, e.g., Ref. [30]), we can also interpret qualitatively the drift of the vortex along the phase gradient as advection of the vortex by flow of the underlying background field. Analogously, the vortex glide along the isophotes of the background field amplitude can be interpreted as a Magnus shift. That the origin of vortex dynamical effects may be justified in this way imparts a generality to the equation of motion, suggesting that it may retain some validity even outside the specific parameters set in its formal derivation.

4. Experimental results and discussions

Experiments were undertaken to measure the motion of a vortex during nonlinear propagation and to compare this behaviour with the theory of vortex motion developed in Section 3. The nonlinear medium was comprised of a 20 cm long cell Pyrex cell containing atomic rubidium vapour. A Ti:sapphire laser provided a cw Gaussian beam tuned to one of the hyperfine 5s–5p$_{3/2}$ resonances of the rubidium atom at a wavelength of 780 nm, for a strong nonlinear response to propagation through the cell. The self-defocusing regime was obtained by detuning the laser to the lower frequency region of the resonance. A schematic of this experimental arrangement is shown in Fig. 1. The initial condition was generated by imaging (with a telescopic lens arrangement) the waist of the Gaussian laser beam onto a phase mask, similar to masks used in previous investigations of screw dislocations [35,36], thereby introducing a singly charged phase dislocation into the wavefront. The

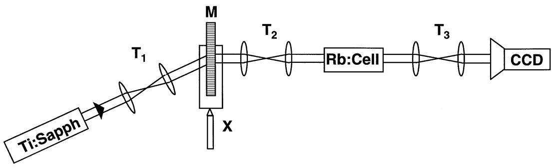

Fig. 1. Experimental setup. Relevant detail may be found in the text. Ti:sapphire denotes the cw laser, T denotes a telescopic lens arrangement, M is the computer generated phase singularity mask from which the first order diffracted beam is taken, X is a translation stage used for direct manipulation of the initial position of the dislocation in the beam, Rb:Cell is the nonlinear medium and CCD is the image capture system.

beam waist and dislocation were then imaged onto the input window of the nonlinear cell. After propagation through the atomic vapour, the image at the output cell window was captured with a CCD camera. Fig. 2(b) shows the output images of a defocused laser beam containing an optical vortex and the associated input profile [Fig. 2(a)], comprised of a Gaussian beam and phase dislocation, from which the vortex soliton was generated. The dark spot in the intensity distribution is coupled to the location of the phase singularity within the spiral wavefronts, and its minimum indicates the location of the optical vortex.

Systematic measurements were made for a beam with an input $1/e^2$ radius of 0.16 mm and power of 52 mW, with the dislocation located 0.11 mm from the beam axis. The output position of the vortex was plotted as function of the detuning away from the resonance. The results are shown in Figs. 3(a) and 3(b) for a cell temperature of 88°C (squares) and 108°C (crosses). As detuning was increased, the induced nonlinear refractive index followed the expected dispersive behaviour, beginning at zero, reaching a maximum at ~ 0.4 GHz and then decreasing far from the resonance.

To test the predictions of our theory against the experimental results presented in Figs. 3(a) and 3(b), the nonlinear evolution of the background was simulated and the position of the vortex at the output of the cell was obtained by integrating Eq. (27) over the 20 cm propagation distance. The model for saturable defocusing nonlinearity was

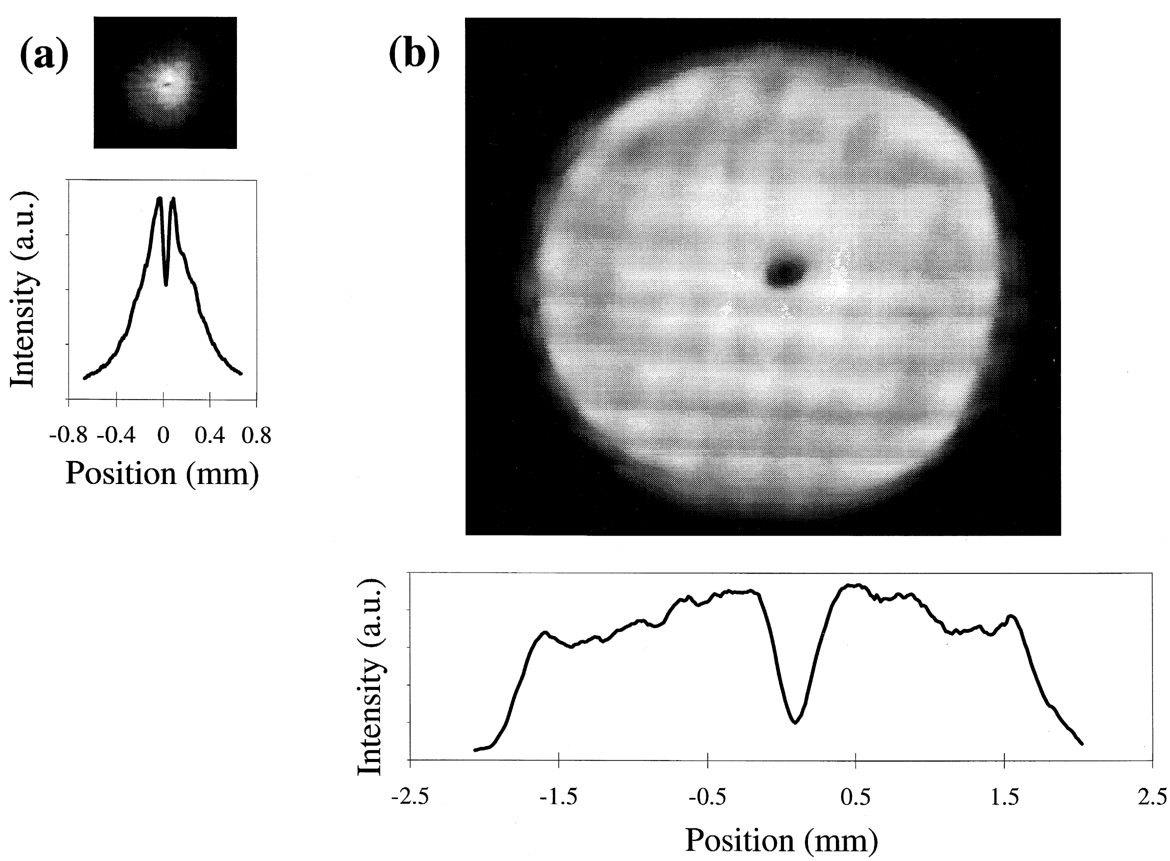

Fig. 2. Examples of optical vortex images captured near the input (a) and just at the output (b) of the cell. Below the images of the corresponding intensity profiles along a line through the vortex are shown. The input profile (a) is comprised of phase dislocation in a Gaussian beam, with linear diffraction producing a dip in the intensity profile. After nonlinear propagation, the optical vortex soliton is formed (b). Magnification factor for (b) is 80% of the magnification factor of (a), as marked by the scales on the profiles.

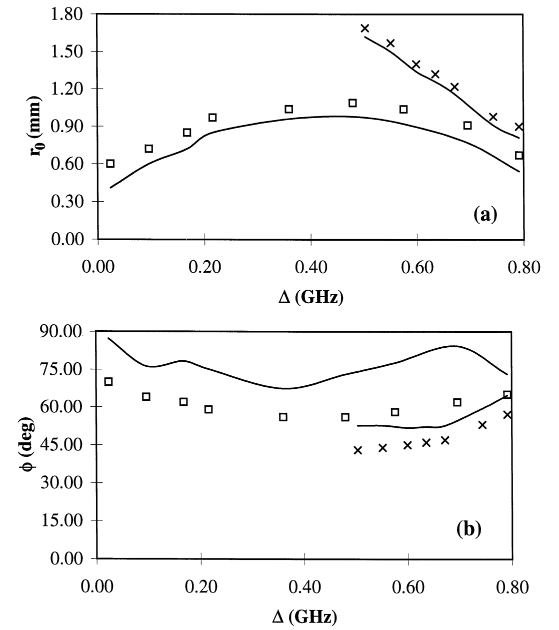

Fig. 3. Output radial (a) and angular (b) position of the vortex at the output of the cell as a function of the detuning below the resonance. The graphs show results for a cell temperature of 88°C (squares) and 108°C (crosses). The corresponding behaviour, predicted by the theory, is shown by the interpolated line. Note that for higher temperature, the vapour concentration is increased thereby strengthening nonlinearity at all detunings.

chosen as in Ref. [5], and model parameters were obtained for each detuning by the process of output profile matching. The output positions predicted by theory are plotted in Figs. 3(a) and 3(b) as solid curves for comparison with experimental results. Similar to the preliminary results previously reported in Ref. [33], Fig. 3(a) shows that the radial motion of the vortex in the beam is very well described by Eq. (27). In addition, Fig. 3(b) shows that there is also a reasonably good qualitative agreement between the theory and experiment with regard to vortex rotation. Discrepancies in the results may arise from transient effects in the beam evolution, in particular the reshaping and radiation associated with the formation of a vortex soliton from a phase dislocation. Such effects were not incorporated in this essentially asymptotic theory for vortex motion.

Fig. 4 shows the results of the asymptotic theory (solid curves) together with numerical simulation results (dashed curves), allowing the vortex propagation dynamics to be directly compared. Nonlinear absorption was removed from the simulations, to allow the propagation conditions to be more closely matched to those under which the asymptotic model (27) was derived. The simulated trajectories followed by the optical vortex follow quite closely the paths calculated from the gradients of the background field. Excellent agreement was obtained for the radial vortex drift in the cases of both Kerr and saturable nonlinearity, see Fig. 4(a). As was the case with experimental results, it was found that the agreement remained qualitatively good provided that the background gradients were shallow over the trajectory of the vortex, i.e. when $|\nabla\theta_b|$, $|\nabla \ln I_b| \ll k_0 n_0 \sqrt{2 n_{nl}(I_0)/n_0}$.

Using the experimental results and the analytical model (27) for the vortex motion driven by varying gradients of the background field, it is possible to suggest a vortex steering mechanism whereby a weak, secondary beam, co-propagating and coherent with the vortex field, is used to manipulate the vortex position. Indeed, this weak beam allows us to vary the background gradients, namely by interferometrically inducing a small initial displacement of the vortex core with respect to the axis of its host beam, and therefore to move the vortex core in the desired direction.

Such a scheme of the vortex steering has been recently demonstrated by us in Ref. [33] where a weak coherent field, with about 1% of the maximum intensity of the vortex background, was split from the laser beam prior to the vortex mask, and recombined near the cell input using a second beam splitter. The weakly interfering beam induced a small change in position of the vortex, with

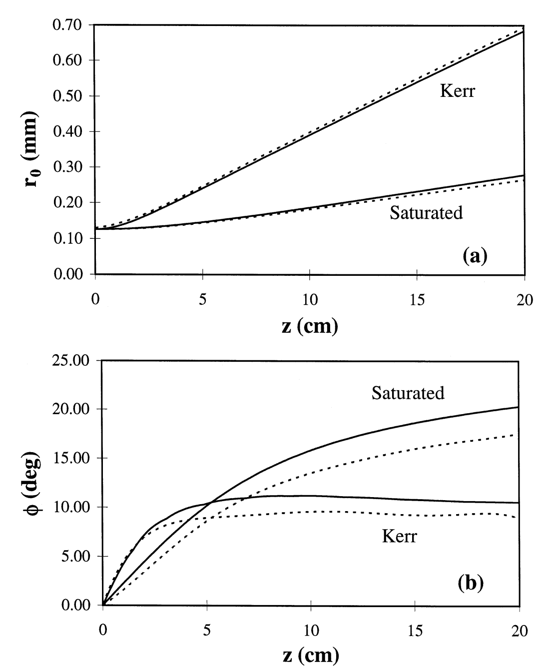

Fig. 4. Radial (a) and angular (b) position of the vortex shown as a function of propagation distance through a simulated absorptionless medium. The graphs show the simulated vortex trajectory (dashed line) along with the theoretical trajectory (solid line) given by the equation of vortex motion (27). Results are shown for both a Kerr medium and a saturable medium, demonstrating applicability of the theory in both cases.

respect to the beam axis, without the destruction of the Gaussian form of the vortex host beam by interference fringes. The amplitude of the interfering field controlled the initial radial displacement of the vortex, $r_0(0)$, while the phase controlled the angular position, $\phi(0)$. The weak field, producing a small initial shift of the vortex radial position, induced a much larger shift after nonlinear propagation, as may be seen from Eq. (30). This allowed the input port of the vortex-induced waveguide to remain approximately fixed, while the output port was steered by the coherent background field, the effect was found to be in excellent agreement with the measured increase in the vortex displacement. These results show that the model we derived here is well suited for describing the steering behaviour of the vortex in a practical context.

5. Conclusion

We have presented an asymptotic theory of the vortex motion in a slowly diffracting background field. We have derived the motion equation for the vortex core which allows us to treat quantitatively the vortex radial drift and rotation induced by the background phase and intensity gradients, respectively. The analytical and numerical results have been compared with experimental data on the vortex drift and rotation in a Gaussian beam passed through a nonlinear medium and good agreement was observed. The results allowed us to suggest and verify a simple scheme for steering optical vortex solitons.

Acknowledgements

Yuri Kivshar would like to thank Igor Aranson, Fernando Lund, and Victor Steinberg for discussions of the theory of vortex motion in superconductors and fluids, and A.A. Nepomnyashchy and A.W. Snyder for some useful remarks and suggestions. Jason Christou would like to thank Eugene Gamaly for fruitful discussions on the general behaviour of wavefront dislocations. The authors are indebted to the referees for useful comments and additional references. L.M.P. acknowledges support from the Fund for Promotion of Research at the Technion and Minerva Center for Nonlinear Physics of Complex Systems.

References

[1] V.E. Zakharov, A.B. Shabat, Zh. Eksp. Teor Fiz. 64 (1973) 1623 [Sov. Phys. JETP 37 (1973) 823]; A. Hasegawa, F. Tappert, Appl. Phys. Lett. 23 (1973) 171.
[2] Ph. Emplit, J.P. Hamaide, F. Reynaud, G. Froehly, A. Barthelemy, Optics Comm. 62 (1988) 374; D. Krökel, N.J. Halas, G. Giuliani, D. Grishkowsky, Phys. Rev. Lett. 60 (1988) 29; A.M. Weiner, J.P. Heritage, R.J. Hawkins, R.N. Thurston, E.M. Kirshner, D.E. Leaird, W.J. Tomlinson, Phys. Rev. Lett. 61 (1988) 2445.
[3] G.A. Swartzlander Jr., D.R. Andersen, J.J. Regan, H. Yin, A.E. Kaplan, Phys. Rev. Lett. 66 (1991) 1583.
[4] E.A. Kuznetsov, S.K. Turitsyn, Zh. Eksp. Teor. Fiz. 94 (1988) 119 [Sov. Phys. JETP 67 (1988) 1583].
[5] V. Tikhonenko, J. Christou, B. Luther-Davies, Yu.S. Kivshar, Optics Lett. 21 (1996) 1129.
[6] A.V. Mamaev, M. Saffman, A.A. Zozulya, Phys. Rev. Lett. 76 (1996) 2262.
[7] Z. Chen et al., Optics Lett. 21 (1996) 629, 716; J. Opt. Soc. Am. B 14 (1997) 3066.
[8] G.S. McDonald, K.S. Syed, W.J. Firth, Optics Comm. 94 (1992) 469; 95 (1992) 281.
[9] C.T. Law, G.A. Swartzlander Jr., Optics Lett. 18 (1993) 586.
[10] D.E. Pelinovsky, Yu.A. Stepanyants, Yu.S. Kivshar, Phys. Rev. E 51 (1995) 5016.
[11] L.P. Pitaevskii, Zh. Eksp. Teor. Fiz. 40 (1961) 646 [Sov. Phys. JETP 13 (1961) 451].
[12] A.W. Snyder, L. Poladian, D.J. Mitchell, Optics Lett. 17 (1992) 789.
[13] G.A. Swartzlander Jr., C.T. Law, Phys. Rev. Lett. 69 (1992) 2503.
[14] B. Luther-Davies, R. Powles, V. Tikhonenko, Optics Lett. 19 (1994) 1816.
[15] G. Duree, M. Moroin, G. Salamo, M. Segev, B. Crosignani, P. Di Porto, E. Sharp, A. Yariv, Phys. Rev. Lett. 74 (1995) 1978.
[16] S. Baluschev, A. Dreischuh, I. Velchev, S. Dinev, Phys. Rev. E 52 (1995) 5517.
[17] Z. Chen, M. Segev, D.W. Wilson, R.E. Muller, P.D. Maker, Phys. Rev. Lett. 78 (1997) 2948.
[18] Z. Chen, M. Shih, M. Segev, D.W. Wilson, R.E. Muller, P.D. Maker, Optics Lett. 22 (1997) 1751.
[19] B. Luther-Davies, J. Christou, V.V. Tikhonenko, Yu.S. Kivshar, J. Opt. Soc. Am. B 14 (1997) 3045.
[20] D. Rozas, C.T. Law, G.A. Swartzlander Jr., J. Opt. Soc. Am. B 14 (1997) 3054.
[21] V.V. Tikhonenko, Yu.S. Kivshar, V. Steblina, A.A. Zozulya, J. Opt. Soc. Am. B 15 (1998) 79.
[22] B.Y. Rubinstein, L.M. Pismen, Physica D 78 (1994) 1.
[23] Yu.S. Kivshar, X. Yang, Optics Comm. 107 (1994) 93.
[24] J.C. Neu, Physica D 43 (1990) 385.
[25] L.M. Pismen, J.D. Rodriguez, Phys. Rev. A 42 (1990) 2471.
[26] L.M. Pismen, J. Rubinstein, Physica D 47 (1991) 353.
[27] R.J. Donnelly, Quantized Vortices in Helium II, Cambridge University Press, Cambridge, 1991.
[28] F.S. Roux, J. Opt. Soc. Am. B 12 (1995) 1215.
[29] K. Staliunas, Chaos, Solitons Fractals 4 (1994) 1783.
[30] C. Nore, M.E. Brachet, S. Fauve, Physica D 65 (1993) 154.
[31] K. Staliunas, Optics Comm. 90 (1992) 123.
[32] V.S. Butylkin, A.E. Kaplan, Yu.G. Khronopulo, E.I. Yakubovich, Resonant Nonlinear Interactions of Light with Matter, Springer, Berlin, 1989.
[33] J. Christou, V. Tikhonenko, Yu.S. Kivshar, B. Luther-Davies, Optics Lett. 21 (1991) 1649.
[34] G. Indebetouw, J. Mod. Optics 40 (1993) 73.
[35] V.Yu. Bazhenov, M.V. Vasnetsov, M.S. Soskin, Pis'ma Zh. Eksp. Teor. Fiz. 52 (1990) 1037 [JETP Lett. 52 (1990) 429].
[36] N.R. Heckenberg, R. McDuff, C.P. Smith, A.G. White, Optics Comm. 94 (1992) 221.